Relaxation modes of an adhering bilayer membrane

Martin Kraus, Udo Seifert

Classification
Physics Abstracts
82.70 — 68.10 — 87.45

Relaxation modes of an adhering bilayer membrane

Martin Kraus and Udo Seifert

Institut für Festkörperforschung, Forschungszentrum Jülich, 52425 Jülich, Germany

(Received 24 March 1994, accepted 7 April 1994)

Abstract. — We determine the relaxational dynamics of the shape fluctuations of a fluid membrane in the vicinity of a substrate. Extending the "classical" description, we include the coupling between the local shape and the difference of the two monolayer densities as well as a lateral tension in the membrane. These extensions introduce additional length scales to the problem. The asymptotic behavior of the dispersion relation and the correlation functions can be understood from limiting cases in which either a free bilayer or a bound incompressible membrane is considered. In many cases, however, the relevant length scales do not separate very well, so that the full dispersion relation will be needed for the interpretation of experiments. It is shown that in addition to the damping due to bulk viscosity the dissipation due to friction between the monolayers is observable and indeed dominates the long-time behavior of the dynamical height correlation function for large wave vectors. As demonstrated with typical sets of parameters, the transition to this regime will be accessible by optical techniques only for weak adhesion and strong friction between the monolayers.

1. Introduction.

One of the earliest phenomena to receive attention in the study of the physical properties of biological membranes [1, 2] has been the slow relaxational dynamics of thermally excited membrane shape fluctuations, such as the "flicker" phenomenon of red blood cells [3]. Fluid phospholipid membranes, although lacking a cytoskeleton and membrane proteins, serve as simple model systems for biological membranes, and are experimentally accessible in form of giant vesicles. These vesicles also exhibit strong shape fluctuations which for free, quasispherical vesicles have been used to determine the bending rigidity, which is the essential material parameter of lipid membranes [4-6]. In addition, the dynamical correlations of these fluctuations give information about the main dissipative mechanisms.

The effect of adhesion or interaction with a substrate on these membranes can be studied in an experimental set-up recently developed by Rädler and Sackmann [7-9]. They have shown that one can obtain the static and dynamic height correlation functions of the bound part of an adhering giant vesicle using reflection interference contrast microscopy.

In the "classical" model of a free membrane, the membrane is treated as a single, incompressible fluid sheet, whose energy is solely determined by the resistance to bending [10], and for which the damping is provided by the surrounding viscous fluid [3]. Three modifications to this classical treatment of the bending modes of a membrane are necessary to represent the experimental situation of an adhering membrane.

First of all, the presence of a substrate modifies the static fluctuation spectrum as well as the hydrodynamics [11, 12]. Secondly, the membrane will be part of a bound vesicle. For wave-lengths much smaller than the size of the vesicle (where up to 50 μm are accessible), the geometrical complications of the closed shape should not affect the dynamics. Therefore, results obtained for a bound *planar* membrane should apply provided the constraints on vesicle volume and area are effectively included in the description as a finite tension in the membrane [13, 14].

Finally, recent work on the equilibrium shapes of vesicles has demonstrated the relevance of the coupling between the local curvature and the local density of lipids within the two monolayers [15]. For static phenomena such as the equilibrium shapes of vesicles, this effect adds an additional *global* energy term, the area-difference-elasticity [16-19]. In the dynamics, bending is coupled to differences in the *local* lipid density in the monolayers, because bending the membrane will compress the inner and stretch the outer monolayer. Since the lipid monolayers are free to slide over each other, these density differences may relax [15, 20]. Thus, the friction between monolayers will provide an additional dissipative mechanism for the damping of undulations [21]. In the small-q regime, the density difference relaxation is too fast to have any effect on the height correlations. For undulations with a sufficiently large wave-vector q, however, the relaxation rate of the monolayer density difference, which scales as q^2, will always be slower than the relaxation of undulations, which scales as q^3 [3]. Due to the coupling between curvature and density, in this regime undulations will relax by a fast process only to the extent that they minimize the energy for given density difference. The slow decay of this density difference then dominates the long-time behavior of the height correlations.

The aim of this work is to combine these three aspects in order to explore the full dynamical behavior of a lipid bilayer membrane near a wall. In particular, we are interested in the circumstances, under which the density relaxation makes an observable contribution to the height fluctuations. One therefore needs to know not only the dispersion relation but also the time-dependent correlation function for the height variable. These quantities inevitably have a rich structure due to the presence of four length-scales. Two length-scales follow from the *static* correlation function in which the potential, the tension and the bending energy all scale differently with the wave-vector. As a third length-scale, the separation from the wall affects the *dynamics*. Finally, the fourth length-scale arises from the coupling to the density difference. Since for a bound membrane, in contrast to the free bilayer, the relaxation rate of the height correlations can become faster than the density relaxation also for small q, one might first expect that the double layer aspect of the membrane is then relevant for all q. However, we will show that the density mode will be observable in the height correlation function only if the undulation energy is dominated by the resistance to bending. For small tension, i.e. weak adhesion, the cross-over to this regime is in the visible range and the coupling to the local density difference should, indeed, have observable effects for a bound membrane.

The paper is organized as follows. In section 2, the general framework of the calculation is set up. We develop the solution of the full problem starting from limiting cases. In section 3, we discuss the free bilayer, for which we here also calculate the time-dependent correlation functions. In section 4, we briefly review the relaxation rate for a bound membrane if the bilayer aspect is ignored. From these two limiting cases, the numerical results for the full problem can be understood. Rather than discussing the dispersion relation and the corresponding

correlation function for all possible cases, we present these quantities for three experimentally motivated examples in section 5. Section 6 contains the conclusion. In Appendix A, the lengthy matrix entries which are the basis for the numerical calculations are given for future reference. In Appendix B, we justify the low Reynolds number approximation. Appendix C deals with the modifications which arise for a typical experimental situation where the fluctuations are measured within a linear strip. In Appendix D, we discuss the effect of finite slip at the substrate as well as the possibility of another slow mode occurring for multilamellar vesicles. Brief accounts of the dispersion relations for the two limiting cases have been presented in references [11, 21].

2. Statics and dynamics of a bound bilayer.

In order to calculate the relaxation modes for both height and monolayer density fluctuations, we first recall the energy of a bilayer. The lipid densities at the neutral surface of each monolayer, $\phi^{\pm}$, have an equilibrium value ϕ_0 for a flat membrane (in this paper (+) will generally denote the monolayer opposite to the wall and (−) the monolayer facing the wall). It is useful to project these densities within each monolayer to a common surface, the bilayer midsurface. These projected densities, $\psi^{\pm}$, will deviate from $\phi^{\pm}$ if the membrane is bent. With H as the mean curvature of the bilayer and d as the distance between the midsurface of the bilayer and the neutral surface of a monolayer, this relation reads $\phi^{\pm} \approx \psi^{\pm}(1 \pm 2dH)$ to lowest order in dH. Expressed in terms of a scaled density deviation from the equilibrium value, $\rho^{\pm} \equiv (\psi^{\pm}/\phi_0 - 1)$, the elastic energy density of each monolayer, $f^{\pm}$, is then given by

$$f^{\pm} = \frac{k}{2}\left(\frac{\phi^{\pm}}{\phi_0} - 1\right)^2 = \frac{k}{2}\left(\rho^{\pm} \pm 2dH\right)^2 \left(1 + O(dH) + O(\rho^{\pm})\right), \tag{1}$$

where k is the area compression modulus of a monolayer [21].

We consider a membrane bound by a potential $V(l)$ whose minimum is at a distance l_0 from a planar wall [22]. Denoting the local displacement of the membrane by $h(x,y) \equiv l(x,y) - l_0$, we can express the mean curvature for small displacements as $H = \frac{1}{2}\nabla^2 h$. The continuum free energy, F, for the entire membrane then is a functional of the membrane shape, $h(x,y)$, and the two densities $\rho^{\pm}(x,y)$,

$$F = \frac{1}{2}\int \mathrm{d}x\,\mathrm{d}y\,\left\{\kappa(\nabla^2 h)^2 + \Sigma(\nabla h)^2 + \Omega h^2 + k\left[(\rho^+ + d\nabla^2 h)^2 + (\rho^- - d\nabla^2 h)^2\right]\right\}. \tag{2}$$

The first three terms represent the energy of undulations at relaxed densities. This energy is given by the bending energy of each monolayer with the usual bilayer bending rigidity κ [10], a tension Σ, which arises from the constraints on area and volume of the vesicle [13, 14], and the contribution from the potential, which we expand about its minimum at $l = l_0$ with $\Omega = \mathrm{d}^2V/\mathrm{d}l^2|_{l=l_0}$. Within the range of wave-lengths accessible by optical methods, these tensions typically can become as relevant as the bending rigidity [23].

For small deviations from the planar state, we consider a plane wave in the x-direction, $h(x,y) \equiv h_q \mathrm{e}^{\mathrm{i}qx}$ and $\rho^{\pm}(x,y) \equiv (\bar{\rho}_q \pm \rho_q)\mathrm{e}^{\mathrm{i}qx}$, written in terms of the difference, $\rho \equiv (\rho^+ + \rho^-)/2$, and the average, $\bar{\rho} \equiv (\rho^+ - \rho^-)/2$, of the scaled projected densities of the monolayers. In the Fourier-transformed free energy,

$$F = \frac{1}{2}\left(h_q, \rho_q, \bar{\rho}_q\right)\mathbf{E}(q)\begin{pmatrix} h_q \\ \rho_q \\ \bar{\rho}_q \end{pmatrix}^*, \tag{3}$$

where we have defined

$$\mathbf{E}(q) \equiv \begin{pmatrix} \tilde{\kappa}\, q^4 + \Sigma\, q^2 + \Omega & -2\, k d q^2 & 0 \\ -2\, k d q^2 & 2\, k & 0 \\ 0 & 0 & 2\, k \end{pmatrix}, \tag{4}$$

$\bar{\rho}$ decouples from h and ρ. The star denotes complex conjugation. Here

$$\tilde{\kappa} = \kappa + 2 d^2 k \tag{5}$$

is a renormalized bending rigidity which includes the effects of elastic deformation of the monolayers. Note that integrating out the density variables, which on the Gaussian level is equivalent to minimizing with respect to them, one recovers the undulation energy of a bound incompressible membrane with

$$F_0 \equiv \min_{\{\rho_q, \bar{\rho}_q\}} F = \frac{1}{2} h_q \left(\kappa q^4 + \Sigma q^2 + \Omega\right) h_q^* \equiv \frac{1}{2} h_q E_0(q) h_q^* . \tag{6}$$

The static correlation functions can be obtained from the inverse of the energy matrix $\mathbf{E}$, which leads to

$$\begin{aligned} \mathbf{G_0}(q) \equiv \left\langle \begin{pmatrix} h_q \\ \rho_q \\ \bar{\rho}_q \end{pmatrix} (h_q, \rho_q, \bar{\rho}_q)^* \right\rangle_0 &= \frac{k_B T}{L_x L_y} \mathbf{E}^{-1}(q) \\ &= \frac{k_B T}{L_x L_y\, E_0(q)} \begin{pmatrix} 1 & d q^2 & 0 \\ d q^2 & E_{hh}(q)/2\, k & 0 \\ 0 & 0 & E_0(q)/2\, k \end{pmatrix} \end{aligned} \tag{7}$$

where L_x and L_y denote the linear dimensions of the rectangular patch of membrane under consideration.

For the calculation of the dynamical correlation functions, we have to consider the hydrodynamics of both the fluid bilayer and the surrounding aqueous solution. The physical properties of the membrane and its undulation energy will enter the boundary conditions and the force balance at the membrane.

The hydrodynamics of the incompressible bulk fluid is treated within the Stokes approximation,

$$\boldsymbol{\nabla} \cdot \mathbf{v} = 0 \qquad \text{and} \qquad \eta \boldsymbol{\nabla}^2 \mathbf{v} = \boldsymbol{\nabla} p \qquad \text{for} \qquad z \neq l_0 . \tag{8}$$

This approximation, neglecting the inertial and advection terms of the Navier-Stokes equation, is valid for low Reynolds numbers, an assumption which has to be checked afterwards (see Appendix B).

We again assume plane waves in the x-direction, with velocity $\mathbf{v} = (v_{q,x}(z)\mathbf{e}_x + v_{q,z}(z)\mathbf{e}_z)\mathrm{e}^{\mathrm{i}qx}$ and pressure $p = p_q(z)\mathrm{e}^{\mathrm{i}qx}$ The general solution to the hydrodynamic equations (8) satisfying the condition of vanishing velocity at the wall and at infinity then is

$$\begin{aligned} v_{q,z}^-(z) &= \left[A\left(\sinh(qz) - qz\cosh(qz)\right) + Bqz\sinh(qz)\right], \\ p_q^-(z) &= 2\eta q\left[-A\cosh(qz) + B\sinh(qz)\right], \\ v_{q,z}^+(z) &= \left[C\mathrm{e}^{-q(z-l_0)} + Dq(z-l_0)\mathrm{e}^{-q(z-l_0)}\right], \\ p_q^+(z) &= 2\eta q D\mathrm{e}^{-q(z-l_0)}, \end{aligned} \tag{9}$$

where the indices $\pm$ apply to $z \gtrless l_0$, respectively, and $v^{\pm}_{q,x}(z) = i\partial_z v^{\pm}_{q,z}(z)/q$. The constants A, B, C, and D are to be determined by boundary conditions at the membrane, which for small displacements may be evaluated at $z = l_0$: the normal velocity v_z has to be continuous, whereas assuming a no-slip boundary condition between lipid and water means that $v^{\pm}_x(l_0)$ has to coincide with the velocities of the lipid flow within the monolayers. Furthermore, the forces have to balance in the normal direction at the membrane, leading to

$$-T^{+}_{zz} + T^{-}_{zz} = -\frac{\partial F}{\partial h^{*}_q}\,, \tag{10}$$

where we have introduced the liquid stress tensor $T^{\pm}_{ij} \equiv -p\delta_{ij} + \eta(\partial_i v_j + \partial_j v_i)$, evaluated at the upper and lower monolayers. Denoting the monolayer surface pressures with $\sigma^{\pm}$, the membrane surface viscosity with μ, and the interlayer friction (whose order of magnitude can be estimated from experiments as in Refs. [24, 15]) with b, the lateral force balance at the two monolayers reads

$$-\widetilde{\nabla}\sigma^{\pm} \pm T^{\pm}_{xz} + \mu\widetilde{\nabla}^2\widetilde{\mathbf{v}}^{\pm} \mp b(\widetilde{\mathbf{v}}^{+} - \widetilde{\mathbf{v}}^{-}) = 0\,. \tag{11}$$

The tilde refers to two-dimensional quantities. At this point, we neglect the fact that the various forces act in different surfaces of the monolayer, e.g. the intermonolayer friction in the bilayer midplane, and the coupling to bulk water at the lipid headgroups. A more sophisticated treatment including this effect should then also incorporate orientational degrees of freedom of the lipids within the monolayer, which are excited by the torques produced in this way.

Equations (10) and (11) and the boundary conditions are sufficient to solve for all of the amplitudes A, B, C, and D of both the flow field $\mathbf{v}(x,z)$ and the pressure $p(x,z)$ as a function of h_q, ρ_q and $\bar{\rho}_q$. Using the assumption of impermeability of the lipid membrane to water flow [25], i.e. $\mathrm{d}h_q/\mathrm{d}t = v_{q,z}(l_0)$, and the continuity equations for the monolayer densities, $\partial_t \rho^{\pm}_q \approx -\widetilde{\nabla}\cdot\widetilde{\mathbf{v}}^{\pm}_q$, which are correct when neglecting the slow lipid flip-flop between the monolayers, we obtain the relaxational dynamics in the form

$$\frac{\mathrm{d}}{\mathrm{d}t}\begin{pmatrix} h_q \\ \rho_q \\ \bar{\rho}_q \end{pmatrix} = -\mathbf{\Gamma}(q, l_0)\mathbf{E}(q)\begin{pmatrix} h_q \\ \rho_q \\ \bar{\rho}_q \end{pmatrix} \tag{12}$$

The explicit expression for the matrix of kinetic coefficients $\mathbf{\Gamma}$, which together with the energy matrix $\mathbf{E}$ contains the full information about the dynamics, is given in Appendix A. Note that this matrix couples the average density $\bar{\rho}_q$ to both h_q and ρ_q. We can now calculate the relaxation times as the inverse values of the eigenvalues γ_i of $\mathbf{\Gamma}\cdot\mathbf{E}$. As shown in Appendix A, the dynamical correlation functions can thus be expressed in the form

$$\langle h_q(t)h^{*}_q(0)\rangle = \langle h_q h^{*}_q\rangle_0 \sum_{i=1}^{3} A^{h}_i \mathrm{e}^{-\gamma_i(q)t} \tag{13}$$

$$\langle \rho_q(t)\rho^{*}_q(0)\rangle = \langle \rho_q \rho^{*}_q\rangle_0 \sum_{i=1}^{3} A^{\rho}_i \mathrm{e}^{-\gamma_i(q)t}\,, \tag{14}$$

Here, $\langle .. \rangle_0$ are the static correlation functions given by equation (7), and the amplitudes $A^{h,\rho}_i$ sum up to unity, $\sum_i A^{h}_i = \sum_i A^{\rho}_i = 1$, to ensure the fluctuation-dissipation-theorem. The explicit expressions for $\mathbf{\Gamma}$ are too complex to allow for an analytical calculation of the eigenvalues and eigenvectors of $\mathbf{\Gamma}\cdot\mathbf{E}$. It turns out, however, that most of the numerical results for the full problem can be understood in terms of two previously considered limiting cases [21, 11, 12].

3. Free bilayer membrane.

The case of a free bilayer membrane, which formally corresponds to $l_0 \to \infty$, has been investigated in reference [21]. We will recall the results briefly, and, as a new result, calculate the correlation functions for this case. Due to the up-down symmetry, the fluctuations of the density average $\bar{\rho}$ decouple from h and the density difference ρ. The matrix of kinetic coefficients for h and ρ is diagonal,

$$\mathbf{\Gamma}^{\mathrm{f}}(q) \equiv \begin{pmatrix} 1/4\eta q & 0 \\ 0 & \dfrac{q^2}{2(2b + 2\eta q + \mu q^2)} \end{pmatrix} \tag{15}$$

while the energy matrix $\mathbf{E}^{\mathrm{f}}$ is just the upper left (2×2) submatrix of $\mathbf{E}$ as defined in equation (4).

The product $\mathbf{\Gamma}^{\mathrm{f}}(q)\mathbf{E}^{\mathrm{f}}(q)$ has two eigenvalues $\gamma^{\mathrm{f}}_{1,2}(q)$, which yield the dispersion relations shown in figure 1a. For simplicity, in this section, we discuss only the case of vanishing tension. There are three regimes [21], separated by the crossover wavevectors $q^{\mathrm{f}}_1 \equiv 2\eta k/b\kappa$ [26] and $q^{\mathrm{f}}_2 \equiv \sqrt{2b/\mu}$,

$$\gamma^{\mathrm{f}}_1 \approx \begin{cases} \dfrac{\kappa}{4\eta} q^3, & q \ll q^{\mathrm{f}}_1 \\ \dfrac{k}{2b}\dfrac{\kappa}{\tilde{\kappa}} q^2, & q^{\mathrm{f}}_1 \ll q \ll q^{\mathrm{f}}_2 \\ \dfrac{k}{\mu}\dfrac{\kappa}{\tilde{\kappa}}, & q^{\mathrm{f}}_2 \ll q \end{cases} \qquad \gamma^{\mathrm{f}}_2 \approx \begin{cases} \dfrac{k}{2b} q^2, & q \ll q^{\mathrm{f}}_1 \\ \dfrac{\tilde{\kappa}}{4\eta} q^3, & q^{\mathrm{f}}_1 \ll q\,. \end{cases} \tag{16}$$

The amplitudes A^h_i and A^ρ_i of the contribution of the two modes to the correlation functions $\langle h_q(t)h_q(0)\rangle$ and $\langle \rho_q(t)\rho_q(0)\rangle$ (see Eqs. (13), (14)), as calculated numerically, are shown in figure 1b.

For $q \ll q^{\mathrm{f}}_1$, there is the "classical" bending mode of a free membrane damped by bulk viscosity, as given by γ^{f}_1, as well as a second mode due to interlayer friction, which decays fast. The asymptotic behavior of the correlation functions can be derived as follows. Undulations relax only by the slow mode, so $A^h_1 \approx 1$, and A^h_2 is negligibly small, since the height variable is too slow to follow the fast density fluctuations. Density differences between the monolayers, however, relax by both modes. On time scales longer than $1/\gamma^{\mathrm{f}}_2$, the density relaxes as to minimize the free energy for given undulations. This condition, $\partial F/\partial \rho^*_q\big|_{h_q} = 0$, implies $\rho_q = dq^2 h_q$, and therefore

$$\langle \rho_q(t)\rho^*_q(0)\rangle \approx d^2q^4 \langle h_q(t)h^*_q(0)\rangle \approx \frac{k_{\mathrm{B}}Td^2}{L_xL_y\kappa} \mathrm{e}^{-\gamma^{\mathrm{f}}_1 t} = \langle \rho\rho^*\rangle_0 \frac{2kd^2}{\tilde{\kappa}} \mathrm{e}^{-\gamma^{\mathrm{f}}_1 t} \tag{17}$$

From this relation and equation (14) we obtain the coefficient $A^\rho_1 \approx 2kd^2/\tilde{\kappa}$ for long times $t \gg 1/\gamma^{\mathrm{f}}_2$, for which it is determined solely by the coupling to height fluctuations. Consequently, $A^\rho_2 \approx 1 - A^\rho_1 = \kappa/\tilde{\kappa}$, so that the ratio of the amplitudes of both modes in the correlation function is given by the ratio of the two contributions to the renormalized bending rigidity (5).

At q^{f}_1 the two damping rates become comparable, so that for $q \gg q^{\mathrm{f}}_1$ the density relaxation is the slowest mode. Density fluctuations will therefore not be induced by the quickly decaying undulations, so that $A^\rho_1 \approx 1$. Fast height fluctuations take place at unrelaxed density difference, which leads to a renormalization of the bending rigidity from κ to $\tilde{\kappa}$ for the faster mode γ^{f}_2. Height fluctuations induced by density differences relax quickly to $h_q = 2kd\rho_q/\tilde{\kappa}q^2$ (as can

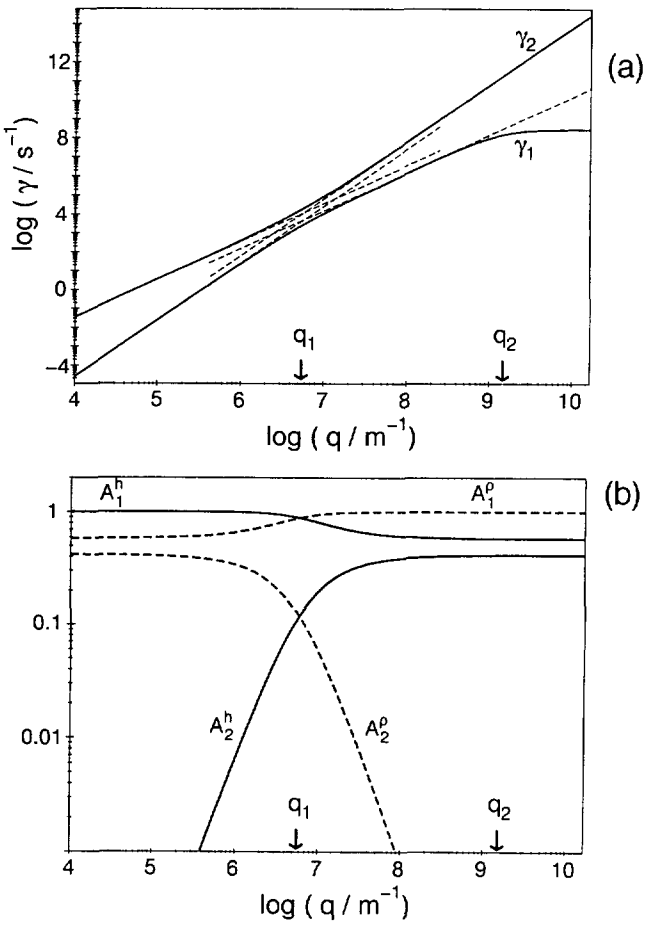

Fig. 1. — (a) Dispersion relations for a free bilayer for $\kappa = 10^{-19}$ J, $k = 0.07$ J/m^2, $d = 1$ nm, $\eta = 10^{-3}$ J s/m^3, $\mu = 10^{-10}$ J s/m^2, and $b = 10^8$ J s/m^4; the dashed lines indicate the asymptotic behavior $\gamma_1 \approx \kappa q^3/4\eta$ and $\gamma_2 \approx kq^2/2b$, for small q; $\gamma_2 \approx \tilde{\kappa} q^3/4\eta$ and $\gamma_1 \approx kq^2\kappa/2b\tilde{\kappa}$, for large q, respectively. (b) Amplitudes of the dynamic correlation functions for a free bilayer as defined in equations (13, 14). The ratio $\kappa/\tilde{\kappa} \simeq 0.417$ determines the asymptotic behavior of both the amplitudes A_2^ρ for small q and A_2^h for large q.

be calculated from $\partial F/\partial h_q^*\big|_{\rho_q} = 0$), which yields $A_1^h \approx 2d^2k/\tilde{\kappa}$, similar to the calculation displayed in equation (17).

Finally, for $q \gg q_2^f$ interlayer friction is replaced by monolayer surface viscosity as the dominant in-membrane damping mechanism in γ_1^f [27]. This crossover, however, does not affect the amplitudes in the correlation function.

An important consequence of these results is that any experiment measuring $\langle h_q(t)h_q(0)\rangle$ will also pick up a contribution from the slow density mode for $q > q_1^f$, provided it is sensitive to the time-scale $1/\gamma_1^f$. In particular, the slowest time-scale in this regime will scale as q^{-2} rather than as q^{-3} In fact, recent measurements of the undulation modes on lipid multilayers using a neutron spin-echo method can be interpreted in this way [28]. For $q \ll q_1^f$, however, the fast membrane-damped mode is *not* visible in the height correlations.

4. Bound membrane without internal modes.

Neglecting the bilayer aspect and the in-plane density modes one finds the relaxational behavior of a bound incompressible membrane as calculated in references [11, 12]. This limit can also be obtained analytically from the full solution as obtained with the formalism of section 2. The damping rate, γ_s, of the single mode can be split in a product of a dynamical part Γ^s and the energy E_0 (cf. Eq. (6)),

$$\gamma^s(q, l_0, \xi_\Sigma, \xi_\kappa) = \Gamma^s(q, l_0) E_0(q, \xi_\Sigma, \xi_\kappa) = \Gamma^s(q, l_0)\ \Sigma \left[\xi_\kappa^{-2} q^4 + q^2 + \xi_\Sigma^{-2}\right] . \tag{18}$$

For wave-vectors below $q = \xi_\Sigma^{-1} \equiv \sqrt{\Omega/\Sigma}$ the dominant contribution to the undulation energy arises from the potential. Above $q = \xi_\Sigma^{-1}$ tension dominates the potential, until bending energy dominates above $q = \xi_\kappa^{-1} \equiv \sqrt{\Sigma/\kappa}$. If the tension is too small to produce a tension-dominated regime, i.e. for $\Sigma < \sqrt{\Omega\kappa}$, there is only one crossover at $q = \xi^{-1}$ with $\xi \equiv (\Omega/\kappa)^{1/4}$.

The hydrodynamical flow fields fall of as q^{-1} perpendicular to the membrane, cf. equation (9). Consequently, for $q < l^{-1}$ the presence of the wall modifies the damping. This crossover shows up in the kinetic coefficient

$$\Gamma^s(q, l_0) \equiv \frac{1}{2\eta q} \frac{\sinh^2(ql_0) - (ql_0)^2}{\sinh^2(ql_0) - (ql_0)^2 + \sinh(ql_0)\cosh(ql_0) + (ql_0)} \tag{19}$$

$$\approx \begin{cases} l_0^3 q^2/12\eta, & q \ll 1/l_0 \\ 1/4\eta q, & q \gg 1/l_0 , \end{cases} \tag{20}$$

where the q^2-dependence for small q can be understood as the effect of conserving the enclosed fluid volume.

Depending on the relative size of the crossover length-scales l_0, ξ_Σ, and ξ_κ, different cases have to be distinguished for the q-dependence of the damping rate γ^s. For $q \ll \min\{l^{-1}, \xi_\Sigma^{-1}, \xi_\kappa^{-1}\}$, one finds

$$\gamma^s \approx \frac{\Omega l_0^3 q^2}{12\eta} \tag{21}$$

The asymptotic behavior for large q is that of a free membrane with $\gamma^s \approx \kappa q^3/4\eta$. In the intermediate regime, the damping rate depends on the relative magnitude of l_0, ξ_Σ and ξ_κ. The asymptotic behavior in the various regimes can then be obtained by multiplication of the respective dominant terms of Γ^s and E_0.

5. Results for the bound bilayer.

In the full problem, the presence of the wall breaks the symmetry between ρ^+ and ρ^- Therefore, the dynamics couples both variables ρ and $\bar{\rho}$ to the fluctuations of h, which leads to three coupled modes. As will be discussed in Appendix B, however, the coupling to the $\bar{\rho}$-mode is typically weak, which allows to discuss the relaxation times and correlation functions for h and ρ as if they were decoupled from $\bar{\rho}$. The remaining two modes are those already discussed above: a hydrodynamic mode arising from the damping of membrane undulations by bulk viscosity and a density mode damped by in-membrane friction.

Due to the number of length-scales involved, there are now many different scenarii for the relaxation rates. Instead of an exhaustive discussion of all possible cases we will discuss the general behavior in terms of the mechanisms explained in the preceding sections for the two limit cases, and present the dispersion relations for three exemplary sets of parameters.

A useful distinction arises from the criterion whether or not there is a crossover vector q_1 separating a small-q regime, where the density adjusts to the height fluctuations, from a large-q regime, where the density cannot follow the fast height fluctuations, whereas the height adjusts to density fluctuations. In analogy to the free bilayer discussed in section 3, such a crossover vector q_1 would be given by the implicit equation

$$\gamma^s(q_1) = \frac{kq_1^2}{2b}, \tag{22}$$

Since γ^s (cf. Eq. (18)) follows regimes not present for the free bilayer, q_1 will in general differ from the value q_1^f. A crossover vector q_1 exists, if the criterion

$$\Omega l_0^3 < 6k\eta/b \tag{23}$$

is fulfilled, as follows from the small-q behavior of γ_s (21).

For any given potential $V(l)$, this criterion can, in principle, be checked. However, it is known from renormalization group calculations on the interaction of membranes with substrates that fluctuations can renormalize such a potential [1, 22], which makes the direct evaluation of criterion (23) difficult. A crude estimate can be obtained as follows. The free parameters on the right side of this criterion are independent of the potential. Typical values are $k = 0.07$ J/m^2, $\eta = 10^{-3}$ J s/m^3, $b = 10^8$ J s/m^4. Since Ωl_0^2 amounts to an adhesion energy V_0, relation (23) becomes $V_0 l_0 < 10^{-12}$ J/m. With typical adhesion energies below 10^{-5} J/m^2, and substrate distances below 100 nm [29, 9] this criterion will thus be met in most physical situations.

We will now discuss the dispersion relations and the correlation functions for three parameter sets. For the first two, the criterion (23) is fulfilled; in the third example we present a case where it is violated.

5.1 FIRST EXAMPLE: SMALL TENSION. — A first example is shown in figure 2: parameters for this case are chosen to follow an experimental example [9]. We consider a giant vesicle in weak adhesion with the fluctuating part facing the wall in an intermediate distance $l_0 \simeq 50$ nm. Tension in such a case is small. The curvature of the potential can be estimated *via* $\Omega = \kappa\xi^{-4}$ (or $\Omega = \Sigma\xi^{-2}$) from the measured real-space correlation length of height fluctuations, which is of the order 0.5 μm. The remaining material parameters as given in the figure caption are chosen as for the free bilayer case.

For $q \ll q_1$, the density difference relaxes quickly and thus follows the undulations. The damping rate for the undulations, as given by γ_1, runs with increasing q through the crossovers ξ_Σ^{-1} and ξ_κ^{-1} already present for a single layer near a substrate, discussed in section 4. Due to the coupling of height and density, the undulations which relax slowly with damping rate γ_1 induce density correlations. These can be calculated analogously to equation (17) with the result

$$A_1^\rho \approx \frac{2kd^2q^4}{\tilde{\kappa}q^4 + \Sigma q^2 + \Omega} \qquad (q \ll q_1). \tag{24}$$

So, for $q \ll \xi_\kappa^{-1}$, A_1^ρ effectively vanishes, and $A_2^\rho \approx 1$, whereas at wave vectors $\xi_\kappa^{-1} < q < q_1$, one observes the low-$q$ behavior of the free bilayer without tension.

The value of $q_1 \simeq (6k\eta/b\kappa l^3)^{1/4}$ is close to l^{-1} in this example. Thus for $q \gg q_1$ one recovers the behavior at $q \gg q_1^f$ of the free bilayer as in section 3. In particular, the relaxation of density differences is too slow to follow the undulations and therefore the bending rigidity is

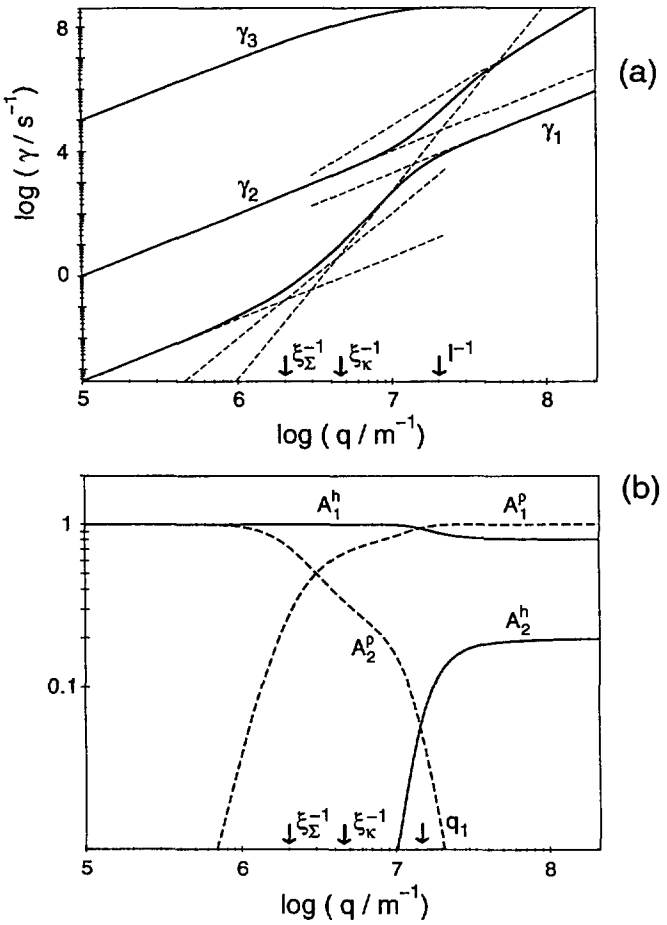

Fig. 2. — (a) Dispersion relations for a bound bilayer; case of weak adhesion and low tension. $\kappa = 0.5 \times 10^{-19}$ J, $k = 0.1$ J/m^2, $d = 1$ nm, $\eta = 10^{-3}$ J s/m^3, $\mu = 10^{-10}$ J s/m^2, $b = 5 \times 10^8$ J s/m^4, $\Omega = 4 \times 10^6$ J, $\Sigma = 10^{-6}$ J/m^2, and $l_0 = 50$ nm; The dashed lines indicate the asymptotic behavior in the various regimes, i.e. $kq^2/2b$ and $\tilde{\kappa}q^3/4\eta$ for γ_2; $\Omega l^3 q^2/12\eta$, $\Sigma l^3 q^4/12\eta$, $\kappa l^3 q^6/12\eta$, and $kq^2\kappa/2b\tilde{\kappa}$ for γ_1. Evaluation of q_1 using the full damping rate from equation (18) gives $q_1 = 1.45 \times 10^7$ m^{-1}. The relaxation mode γ_3 of the average monolayer density $\bar{\rho}$ decays much faster. (b) Amplitudes of the dynamic correlation functions for a bound bilayer as defined in equations (13, 14). Parameters used here give $\kappa/\tilde{\kappa} \simeq 0.2$ for the large-q behavior of A_2^h.

renormalized. As above, it is possible to calculate the asymptotics of the amplitudes of the dynamic correlation function in this regime, giving $A_1^\rho \approx 1$,

$$A_1^h \approx \frac{2kd^2q^4}{\tilde{\kappa}q^4 + \Sigma q^2 + \Omega} \qquad (q \gg q_1)\,, \tag{25}$$

and $A_2^h \approx 1 - A_1^h$. For $q \gg \xi_\kappa^{-1}$, the amplitude A_1^h reduces to $2kd^2/\tilde{\kappa}$.

5.2 SECOND EXAMPLE: LARGE TENSION. — A second example, also motivated by an experimental situation, is presented in figure 3. Here, we consider a pancake-like vesicle which is strongly bound to the substrate. The upper side of such a vesicle is flickering, while the

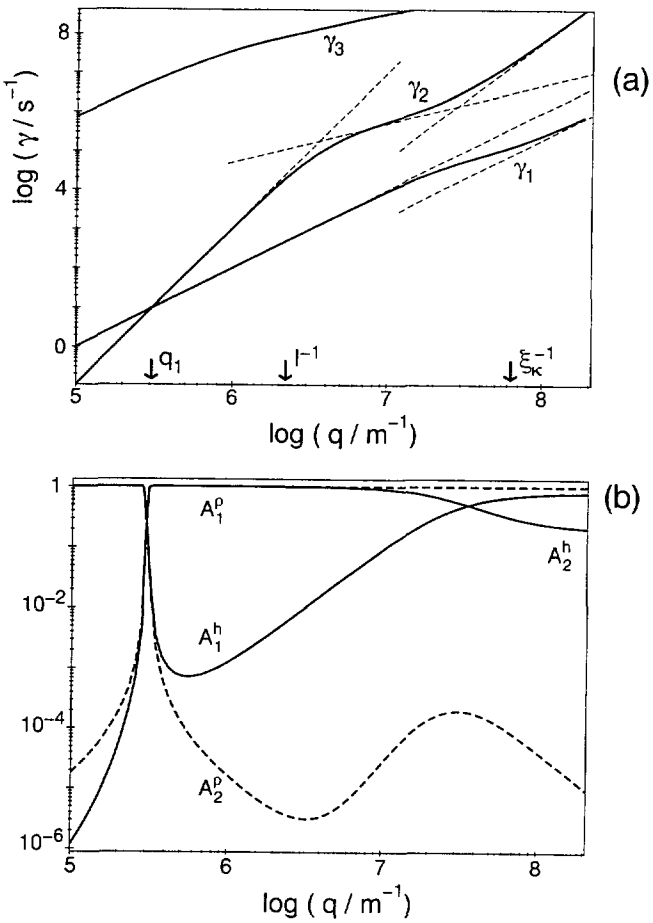

Fig. 3. — (a) Dispersion relations for a bound bilayer; case of large tension. Parameters as in figure 2, except for $\Sigma = 2 \times 10^{-4}$ J/m^2, $l_0 = 400$ nm, $\Omega = 0$. The dashed lines indicate the asymptotic behavior in the various regimes as discussed in the text: the in-membrane damping rate changes from $kq^2/2b$ to $kq^2\kappa/2b\tilde{\kappa}$, while the bulk damping passes the asymptotical behaviors $\Sigma l^3 q^4/12\eta$, $\Sigma q/4\eta$, and $\tilde{\kappa}q^3/4\eta$. (b) Amplitudes of the dynamic correlation functions for a bound bilayer as defined in equations (13, 14). The ratio $\kappa/\tilde{\kappa}$ is as in figure 2, whereas A_1^h is determined by the coupling to density and follows equation (25) for $q \gg q_1$.

lower side is essentially fixed by the strong adhesion. We assume that the no-slip boundary condition at the wall, which now is coated by the fixed bilayer, is still valid (for a modification see Appendix D). Due to the large distance from the wall, the fluctuating membrane will not be held in position by a potential, but rather by the constraints on area and volume of the vesicle. Thus Ω may be neglected. Because of the strong adhesion, tension is large, but should be still one order of magnitude below the lysis tension, which is of the order 10^{-3} J/m^2 [30].

With parameters accordingly chosen as given in the figure caption, $q_1 = \sqrt{6k\eta/b\Sigma l_0^3}$ turns out to be very small, and the length scales q_1, l_0^{-1}, and ξ_κ^{-1} are well separated. For $q \ll q_1$, $A_1^h \simeq A_2^\rho \simeq 1$, since the coupling of density correlations to the slowly decaying undulations follows equation (24) and thus effectively vanishes for $q \ll \xi_\kappa^{-1}$

For $q \gg q_1$ there is a large tension-dominated regime, where the damping changes from

$\gamma_2 \approx \Sigma l^3 q^4/12\eta$ to $\gamma_2 \approx \Sigma q/4\eta$ at $q = l^{-1}$ The height correlations induced by the slow density mode follow equation (25), and thus are negligible for $q \ll \xi_\kappa^{-1}$ Only above $q = \sqrt{\Sigma/\tilde{\kappa}}$ does the (for all $q > q_1$ renormalized) bending rigidity dominate the undulation energy. From the form of A_1^h, (Eq. (25)), it can be seen, that only in this regime the height correlations are influenced by the slow density mode, whose damping rate γ_1 is then shifted by a factor $\kappa/\tilde{\kappa}$. Thus, in this example observable effects of the renormalization of bending rigidity set in at a larger value of q than where the interchange of slow and fast mode takes place, contrary to the free bilayer case.

5.3 THIRD EXAMPLE: SLOW DENSITY RELAXATION FOR ALL q. — If the condition (23) is violated, the density relaxation is always slow and there is no crossover wave-vector q_1. Density differences cannot be induced by fast height fluctuations, resulting in a negligible A_2^ρ. The height correlations induced by the coupling to the slowly decaying density mode, as expressed in A_1^h, are now given by equation (25) for *all* q. As we have seen in the second example, however, this turns out to be an observable effect in the height correlation function, i.e. A_1^h is of order unity, only for $q \gg \sqrt{\Sigma/\tilde{\kappa}}$.

As an example, we consider a charged membrane pushed by a linear potential (e.g. arising from an osmotic pressure) towards the substrate. In weak electrolytes, where the screening length is large compared to l_0, fluctuations beyond the harmonic level can safely be ignored. The potential then reads $V(l) = \pi k_B T/(2l_B l) + pl$, where $l_B \simeq 0.7$ nm is the Bjerrum length in water. For this potential, $\Omega l_0^3 = \pi k_B T/l_B \simeq 1.8 \times 10^{-11}$ J/m is independent of l_0 and indeed violates the criterion (23).

For the relaxation rates, a large Ω means that there will be no tension-dominated regime. The two modes follow the small-q-behavior of $\gamma_s \approx \Omega l_0^3 q^2/12\eta$ (21) and $\gamma_2^f \approx kq^2/2b$ (16), until at $q \gg \{\xi^{-1} \equiv (\Omega/\kappa)^{(1/4)}, l^{-1}\}$ the large-q behavior of the free bilayer is recovered again.

6. Conclusion.

We have calculated the relaxation modes for a bound membrane with additional degrees of freedom due to monolayer density fluctuations employing linearized hydrodynamics. The presence of the wall and the undulation energy contributions by potential and tension give rise to a number of cross-over length-scales and affect not only the damping of undulations, but also the relevance of the coupling of bending and density modes.

The coupling between density and height variables becomes relevant to the height correlation function beyond a cross-over q-vector given by the maximum of q_1 (as defined in Eq.(22)), $1/\xi$ and $1/\xi_\kappa$ (as defined in Sect. 4). Since this cross-over typically is larger than the corresponding value of a free bilayer membrane, the coupling between shape and density will be more difficult to detect for a bound membrane. For typical values, as used in the examples discussed above, this cross-over corresponds to a wave-length which is at the lower end of the optically accessible range (compare Fig. 2) or even smaller as in figure 3.

If the coupling between shape and density can be neglected, the correlation function for the height variable is given by

$$\langle h_q(t) h_q^*(0) \rangle = \frac{k_B T}{L_x L_y (\kappa q^4 + \Sigma q^2 + \Omega)} e^{-\gamma_s(q) t}, \tag{26}$$

with $\gamma_s(q)$ defined in equation (18). Since the tension in the membrane can cause a crossover in the optical range as it happens for weak adhesion shown in figure 2, the relaxation rate does not obey a simple power law for a large q-range. In such a case, a fit against the expression (26) is necessary. This expression contains in $\gamma_s(q)$ two more parameters, namely the viscosity η

and the separation l_0, than the corresponding static correlation functions, i.e. the mean square amplitudes as given by the preexponential factor in (26). Since the viscosity is known, the dynamical measurements could be used to obtain the separation l_0 from these data. Likewise, if this separation is measured independently, the dynamical data provide a much better basis for a determination of the curvature Ω of the adhesion potential and the effective tension Σ.

In any precise determination of these quantities from experimental data, one has to be aware of additional modifications some of which we discuss in Appendices C and D. In Appendix C, we present the correlation functions as appropriate if data have been obtained only for a linear strip. As shown in Appendix D, the relaxation rate will also be slightly modified if the substrate is coated with another bilayer. There we also point out that for multilamellar vesicles a peristaltic mode causes another slow time-scale. As a consequence of all these complications, a quantitative comparison with experimental data available so far [9] has not yet been achieved.

The full analysis presented in this paper will be mandatory for the interpretation of any experiment in the cross-over regime where the height correlation function will show bi-exponential behavior. In the two examples presented here, the two time-scales are well separated even in the cross-over region but different parameter sets may lead to a closer gap between the two modes.

There are, in principle, two possibilities to reach this cross-over regime where the coupling between shape and density becomes relevant. For weak adhesion, which implies weak tension, as shown in figure 2, the cross-over is dominated by q_1, i.e. the value of the friction coefficient b. If the friction is increased, the cross-over would shift towards longer wave-length. One may speculate whether close to the main transition this friction becomes larger due to the freezing of the chains. Likewise in mixtures of lipids with different chain lengths, this friction may be enhanced. Secondly, one could contemplate grazing incidence neutron reflection or, at the present stage even more speculatively, X-ray microscopy, to gain access to wave-vectors beyond 10^7/m. In fact, the recent analysis of a neutron spin echo experiment [28] on a stack of membranes has given strong indication for the relevance of the coupling between height and density difference for $q \simeq 10^8 - 10^9$/m.

Acknowledgments.

We acknowledge stimulating discussions with W. Fenzl, R. Lipowsky, J. Rädler, E. Sackmann and H. Strey.

Appendix A.

Explicit expression for Γ and calculation of modes.

The matrix Γ as defined in equation (12) has been calculated analytically using the computer algebra system Maple [31]. The result for the matrix elements then reads

$$\begin{aligned}\Gamma_{11} = & - \left(-2\mu b q \cosh^2(l_0 q) - 2\eta\mu q^2 \cosh(l_0 q)\sinh(l_0 q) - 2\eta\mu q^2 \cosh^2(l_0 q)\right.\\ & - \mu^2 q^3 \cosh^2(l_0 q) + 2\eta\mu l_0^2 q^4 + 2\eta\mu l_0 q^3 + 4\eta^2 q^2 l_0 + \mu^2 l_0^2 q^5 + 2b\eta l_0 q + 2b\eta l_0^2 q^2\\ & + 2\mu b l_0^2 q^3 + 2\eta b + \mu^2 q^3 + 2\eta\mu q^2 + 2b\mu q - 2b\eta \cosh^2(l_0 q)\\ & \left. - 4\eta^2 q \sinh(l_0 q)\cosh(l_0 q) - 2b\eta \cosh(l_0 q)\sinh(l_0 q)\right) / (\eta q Y_1) \end{aligned} \tag{27}$$

$$\Gamma_{12} = \Gamma_{21} = -(2\eta + \mu q) q^3 l_0^2 / Y_1 \tag{28}$$

$$\Gamma_{13} = \Gamma_{31} = \left(2b + 2\eta q + \mu q^2\right) q^2 l_0^2 \left(\cosh(l_0 q) - \sinh(l_0 q)\right) / Y_2 \tag{29}$$

$$\Gamma_{22} = -q^2\left(-\mu\, l_0 q^2 \sinh(l_0 q) - \mu\, l_0^2 q^3 \cosh(l_0 q)^2 + \mu\, l_0\, q^2 \cosh(l_0 q) + \mu\, l_0^2\, q^3 \sinh(l_0 q) + \eta \cosh(l_0 q) + \mu\, q \sinh(l_0 q) + \eta \sinh(l_0 q)\right) / Y_2 \quad (30)$$

$$\Gamma_{23} = \Gamma_{32} = \eta\, q^2 \left(1 + 2\, l_0^2 q^2 - 2\, l_0 q\right)\left(\cosh(l_0 q) - \sinh(l_0 q)\right) / Y_2 \quad (31)$$

$$\Gamma_{33} = -q\left(\left(\eta\, q + \mu\, l_0^2 q^4 + \mu\, q^2 + 2\, b\, l_0^2 q^2 + 2\, b - 2\, b\, l_0 q - \mu l_0 q^3\right) \sinh(l_0 q) + \left(\eta\, q + \mu\, l_0 q^3 - 2\, b\, l_0^2 q^2 - \mu\, l_0^2 q^4 + 2\, b\, l_0 q\right) \cosh(l_0 q)\right) / Y_2 \quad (32)$$

where we have defined

$$\begin{aligned} Y_1 = {} & 8\eta^2 l_0 q^2 + 4\eta\,\mu\, q^2 - 8\eta^2 l_0^2 q^3 + 4\mu\, b\, l_0^2 q^3 + 4\,\mu\, b\, q - 4\mu\, b\, q \cosh^2(l_0 q) - 4\mu\, b\, l_0 q^2 \\ & - 2\,\mu^2 l_0 q^4 + 2\,\mu^2 l_0^2 q^5 - 8\, b\,\eta \cosh^2(l_0 q) - 8\,\eta^2 q \cosh^2(l_0 q) - 2\,\mu^2 q^3 \cosh(l_0 q) \sinh(l_0 q) \\ & - 8\,\eta\, b \cosh(l_0 q) \sinh(l_0 q) - 2\,\mu^2 q^3 \cosh^2(l_0 q) + 2\,\mu^2 q^3 - 4\,\mu\, b\, q \cosh(l_0 q) \sinh(l_0 q) \\ & - 8\,\eta\,\mu\, q^2 \cosh(l_0 q) \sinh(l_0 q) + 4\,\eta\, b - 8\,\eta^2 q \sinh(l_0 q) \cosh(l_0 q) \\ & - 8\,\eta\,\mu\, q^2 \cosh^2(l_0 q), \end{aligned} \quad (33)$$

$$\begin{aligned} Y_2 = {} & \left(2\, b\,\eta + 4\,\eta^2 l_0 q^2 - 4\,\eta^2 l_0^2 q^3 + \mu^2 q^3 + 2\,\eta\,\mu\, q^2 + 2\,\mu\, b\, l_0^2 q^3 - 2\,\mu\, b\, l_0 q^2 \right. \\ & \left. + 2\,\mu\, b\, q + \mu^2 l_0^2 q^5 - \mu^2 l_0 q^4\right)\, 2 \sinh(l_0 q) \\ & + \left(2\, b\,\eta - 4\,\eta^2 l_0 q^2 + 4\,\eta^2\, q + 4\,\eta^2 l_0^2 q^3 + 2\,\eta\,\mu\, q^2 - 2\,\mu\, b\, l_0^2 q^3 + 2\,\mu\, b\, l_0 q^2 \right. \\ & \left. - \mu^2\, l_0^2 q^5 + \mu^2 l_0 q^4\right)\, 2 \cosh(l_0 q). \end{aligned} \quad (34)$$

Having obtained the matrix of kinetic coefficients, we can now calculate the dynamical correlation functions. A formal solution to the relaxational dynamics, equation (12), is $(h_q, \rho_q, \bar{\rho}_q)(t) = \exp(-\mathbf{\Gamma}\cdot\mathbf{E}\, t)(h_q, \rho_q, \bar{\rho}_q)(0)$. After diagonalization, one obtains the relaxation times of the various modes as the inverse values of the eigenvalues γ_i of $\mathbf{\Gamma}\cdot\mathbf{E}$.

The time-dependent correlation functions can be obtained from the corresponding eigenvectors $\mathbf{g}_i$. The matrix $\mathbf{U} = [\mathbf{g}_1\, \mathbf{g}_2\, \mathbf{g}_3]$ with matrix elements U_{ij} diagonalizes $\mathbf{\Gamma}\cdot\mathbf{E}$. The dynamical correlation matrix $\mathbf{G}(t)$ is defined by

$$\mathbf{G}(t) \equiv \left\langle \begin{pmatrix} h_q \\ \rho_q \\ \bar{\rho}_q \end{pmatrix}(t)\,(h_q, \rho_q, \bar{\rho}_q)^*(0) \right\rangle = \mathrm{e}^{-\mathbf{\Gamma}\cdot\mathbf{E}\, t}\mathbf{G_0} = \mathbf{U} \exp\left(- \begin{bmatrix} \gamma_1 & 0 & 0 \\ 0 & \gamma_2 & 0 \\ 0 & 0 & \gamma_3 \end{bmatrix} t \right) \mathbf{U}^{-1}\mathbf{G_0} \quad (35)$$

In order to obtain the static correlation functions for $t \to 0$ we have used the fluctuation - dissipation - theorem $\mathbf{G}(t=0) = \mathbf{G}_0 = (k_B T / L_x L_y)\,\mathbf{E}^{-1}$ For the matrix elements of $\mathbf{G}(t)$, equation (35) reads

$$\mathbf{G}_{jk}(t) = \sum_i \mathrm{e}^{-\gamma_i t} U_{ji} \sum_m (\mathbf{U}^{-1})_{im} (\mathbf{G_0})_{mk} \quad (36)$$

$$\equiv \sum_i \mathrm{e}^{-\gamma_i t} A_i^{jk} (\mathbf{G_0})_{jk} \quad (37)$$

where the condition $\mathbf{G}(t=0) = \mathbf{G}_0$ is equivalent to $\sum_i A_i^{jk} = 1$. Here, the indices $\{1,2,3\}$ correspond to $\{h, \rho, \bar{\rho}\}$, i.e $\langle h_q(t) h_q^*(0)\rangle = \mathbf{G}_{11}(t)$, and so on. For convenience, we use A_i^h instead of A_i^{11}, and A_i^ρ for A_i^{22}.

Appendix B.

Reynolds numbers and coupling to $\bar{\rho}$.

The Reynolds number, Re, is a measure for the relevance of inertial and advective terms in the Navier-Stokes equation as compared to the friction term. For decaying plane waves it can be

estimated by replacing the spacial derivatives by the wave-vector q, and the time derivative by the relaxation rate γ, leading to $\mathrm{Re} = \rho\gamma/\eta q^2$. Calculating the Reynolds number for the two slowest modes $\gamma_{1,2}$ gives $\mathrm{Re}_{1,2} \ll 1$, thus confirming the validity of the Stokes approximation, (Eq. (8)).

The coupling of h and ρ to $\bar{\rho}$, expressed in the amplitudes of the correlation function A_3^h and A_3^ρ, turns out to be negligible for all reasonable parameter values. These amplitudes are always less than 10^{-5} for the examples discussed in section 5. We conclude that the error we made by treating also this mode within the Stokes approximation should not be harmful to our results. For the $\bar{\rho}$-mode, we find $\gamma_3 \approx 2klq^2/\eta$ for small q, and $\gamma_3 \approx kq/(2\eta + \mu q)$, the result obtainable analytically for the free bilayer as well, for large q. However, these results are non-physical, since the Reynolds number for this mode, estimated as $\mathrm{Re}_3 = \rho\gamma_3/\eta q^2$, turns out to be bigger that 1. A proper treatment of this mode would then reveal oscillatory "sound" modes within the membrane [21].

Appendix C.

Measurement of correlations in a linear strip.

In experiments using video microscopy, membrane displacements are frequently measured in a finite strip of length L parallel to $x = 0$, averaging over the width B of the strip [32, 9]. B will most often be determined by the optical resolution of the microscope. Thus the observed quantity is

$$H(x) = \frac{1}{B}\int_{-B/2}^{B/2} h(x,y)\mathrm{d}y\,. \tag{38}$$

Defining the Fourier transform as $H(x) = \sum_{q_x} H_{q_x}\exp(iq_x x)$, one obtains from equation (38)

$$\langle H_{q_x}^2\rangle = \sum_{q_y}\left\langle h_{(q_x,q_y)}^2\right\rangle \frac{4\sin^2(q_y B/2)}{q_y^2 B^2} \equiv \sum_{q_y}\left\langle h_{(q_x,q_y)}^2\right\rangle K_s(q_y)\,, \tag{39}$$

for the static height correlation function, where the correction factor $K_s(q_y)$ arises from the Fourier-transform of the finite strip. For $q_y \ll B^{-1}$, this factor reduces to unity. Projection on the strip is then equivalent to integration over all possible values of the component of the wave-vector perpendicular to the strip.

For an evaluation, we replace the sum by an integral, $\sum_{q_y} \to (L_y/2\pi)\int_{-\infty}^{\infty}\mathrm{d}q_y$. Using equation (7) for $\left\langle h_{(q_x,q_y)}^2\right\rangle$ we obtain in the limit $B \to 0$

$$\langle H_{q_x}^2\rangle = \begin{cases} \dfrac{k_\mathrm{B}T}{L_x}\dfrac{(\kappa^{1/4}\sin\left(\frac{1}{2}\arccos(C)\right))}{(\Omega + \Sigma\, {q_x}^2 + \kappa\, {q_x}^4)^{1/4}\sqrt{-\Sigma^2 + 4\,\kappa\,\Omega}} & ,\Sigma^2 < 4\kappa\Omega \\ \dfrac{k_\mathrm{B}T}{L_x\sqrt{2\Sigma^2/\kappa - 8\,\Omega}}\left(-\dfrac{\sqrt{|D^+|}}{D^+} + \dfrac{\sqrt{|D^-|}}{D^-}\right) & ,\Sigma^2 > 4\kappa\Omega\,, \end{cases} \tag{40}$$

with

$$C \equiv \frac{\Sigma + 2\,\kappa\,{q_x}^2}{2\sqrt{\kappa}\sqrt{\Omega + \Sigma\,{q_x}^2 + \kappa\,{q_x}^4}}\,, \tag{41}$$

and

$$D^\pm \equiv \Sigma + 2\,\kappa\,{q_x}^2 \pm \sqrt{\Sigma^2 - 4\,\kappa\,\Omega}\,. \tag{42}$$

In the special case without a potential, $\Omega = 0$, this expression has been previously derived by Mutz and Helfrich [32]. For small q_x, the function $\langle H^2_{q_x} \rangle$ is constant. For $\xi_\Sigma^{-1} \ll q_x \ll \xi_\kappa^{-1}$ it behaves as $(\sigma q_x)^{-1}$, and for $q \gg \xi_\kappa^{-1}$ it behaves as $(\kappa q_x)^{-3}$

The expression for the dynamical correlation function in the same geometry yields

$$\langle H_{q_x}(t) H^*_{q_x}(0) \rangle = \frac{L}{2\pi} \int \mathrm{d}q_y \left\langle h_{(q_x,q_y)}(t) h^*_{(q_x,q_y)}(0) \right\rangle = \frac{L}{2\pi} \int \mathrm{d}q_y \left\langle h^2_{(q_x,q_y)} \right\rangle_0 \sum_i A_i^h \mathrm{e}^{-\gamma_i(q_x,q_y)t}, \tag{43}$$

which has to be evaluated numerically. Thus, for every particular wave-vector q_x, a superposition of relaxation rates contributes to the correlation function.

As an example, we have performed the q_y-integration of the dynamical correlation function, equation (43) for the "classical" case of a free membrane without internal degrees of freedom. For $u \equiv \kappa q_x^3 t/4\eta \ll 1$, the result is governed by the static correlations on the strip, $\langle H_{q_x}(t) H^*_{q_x}(0) \rangle \sim t\mathrm{e}^{-u}/4\eta u = \mathrm{e}^{-u}/(\kappa q_x^3)$. However, for $u \gg 1$, we obtain $\langle H_{q_x}(t) H^*_{q_x}(0) \rangle \sim t\mathrm{e}^{-u}/4\eta u^{3/2} = 2\eta^{1/2}\mathrm{e}^{-u}/t^{1/2}(\kappa q_x^3)^{3/2}$, i.e. the correlations on the strip fall off faster with q_x than in $\langle h(q_x, q_y = 0, t) h(q_x, q_y = 0, 0) \rangle$.

Appendix D.

Extensions of the model.

In this section, we want to discuss briefly some simple extensions of the model applying to somewhat modified physical situations. So far, we have assumed a smooth solid wall with no-slip boundary condition. If the interface between substrate and adjacent fluid is coated by another lipid monolayer or bilayer, as is also the case for strongly adhering "pancake" vesicles (see example 2), it may be necessary to allow for a finite slip at $z = 0$. This is done by introducing a friction term $\propto \tilde{b}\, v_x(z=0)$ with a phenomenological friction coefficient $\tilde{b}$ in the force-balance at the substrate that replaces the condition $v_x(z=0) = 0$. It turns out that, for small q, this leads to a correction factor $(4 + \tilde{b}l_0/\eta)/(1 + \tilde{b}l_0/\eta)$ in the damping rate (18) of the undulation mode. The q^2 - dependency of the damping, however, remains valid, since the slip does not change the conservation of volume between membrane and substrate. For coating with a bilayer, we may use $\tilde{b} \simeq b = 10^8$ J s/m^4, which leads for $l_0 \simeq 50$ nm to $\tilde{b}l_0/\eta \simeq 5 \times 10^3$. In this case, the correction due to the slip is negligible. In the low-friction regime, that is for $\tilde{b} \ll l_0/\eta$, the correction can reach a factor of 4.

In experiments, very often multilamellar vesicles are observed. In the case of adhesion, they may be described as a stack of membranes near a wall separated by small amounts of water [33]. Thus, for small q, the flow fields of the membranes affect each other leading to a modification of the damping rates. As a simple example, we consider two membranes without internal degrees of freedom as discussed in section 4. Their distances to the wall will be denoted by l_1 and l_2, respectively, with a mean intermembrane distance $\Delta l \ll \{l_1, l_2\}$. We can expand the membrane-membrane interaction potential $V_\mathrm{m}(l_2 - l_1)$ about Δl, with $\Omega_\mathrm{m} \equiv \mathrm{d}^2 V_\mathrm{m}/\mathrm{d}(l_2 - l_1)^2|_{l_2 - l_1 = \Delta l}$. For $q \ll \xi_\Sigma^{-1}$, the two modes for two independent membranes with $\gamma \approx \Omega l_i^3 q^2/12\eta$ (see Eq. (21); $i = 1, 2$) are replaced by two collective modes. The faster mode has essentially twice the undulation energy of a single membrane, while the second one, the "peristaltic" mode [3], can become very slow with

$$\gamma_1 \approx \frac{\Omega_\mathrm{m}(\Delta l)^3 q^2}{12\eta}, \tag{44}$$

since the length l_t is replaced by Δl. Both modes lead to appreciable height fluctuations and should be visible in optical experiments.

References

[1] Lipowsky R., *Nature* **349** (1991) 475.

[2] The Structure and Conformation of Amphiphilic Membranes, Vol. **66** of Springer Proceedings in Physics, R. Lipowsky, D. Richter and K. Kremer Eds. (Springer, Berlin, 1991).

[3] Brochard F. and Lennon J., *J. Phys. France* **36** (1975) 1035;
Frey E. and Nelson D.R., *J. Phys. I France* **1** (1991) 1715.

[4] Engelhardt H., Duwe H. and Sackmann E., *J. Phys. Lett. France* **46** (1985) L-395.

[5] Bivas I., Hanusse P., Bothorel P., Lalanne J. and Aguerre-Chariol O., *J. Phys. France* **48** (1987) 855.

[6] Duwe H., Käs J. and Sackmann E., *J. Phys. France* **51** (1990) 945.

[7] Zilker A., Engelhardt H. and Sackmann E., *J. Phys. France* **48** (1987) 2139.

[8] Rädler J. and Sackmann E., *J. Phys. II France* **3** (1993) 727.

[9] Rädler J., Ph. D. thesis, TU–München (1993).

[10] Helfrich W., *Z. Naturforsch.* **28c** (1973) 693.

[11] Seifert U., *Phys. Rev. E* **49** (1994) 3124.

[12] Seifert U. and Langer S., *Biophys. Chem.* **49** (1994) 13.

[13] Helfrich W. and Servuss R.-M., *Il Nuovo Cimento* **3D** (1984) 137.

[14] Milner S. and Safran S., *Phys. Rev. A* **36** (1987) 4371.

[15] Evans E., Yeung A., Waugh R. and Song J., The Structure and Conformation of Amphiphilic Membranes, Vol. **66** of Springer Proceedings in Physics, R. Lipowsky, D. Richter and K. Kremer Eds. (Springer, Berlin, 1991) pp. 148-153.

[16] Seifert U., Miao L., Döbereiner H.-G. and Wortis M., The Structure and Conformation of Amphiphilic Membranes, Vol. **66** of Springer Proceedings in Physics, R. Lipowsky, D. Richter and K. Kremer Eds. (Springer, Berlin, 1991) pp. 93-96.

[17] Miao L., Seifert U., Wortis M. and Döbereiner H.-G., *Phys. Rev. E*, in press.

[18] Wiese W., Harbich W. and Helfrich W., *J. Phys.: Cond. Matter* **4** (1992) 1647.

[19] Waugh R., Song J., Svetina S. and Zeks B., *Biophys. J.* **61** (1992) 974.

[20] Fischer T., *Biophys. J.* **63** (1992) 1328.

[21] Seifert U. and Langer S., *Europhys. Lett.* **23** (1993) 71.

[22] Lipowsky R. and Leibler S., *Phys. Rev. Lett.* **56** (1986) 2541.

[23] The modes of an interface with dominating tension are discussed in A. Ammann, U. Seifert, and R. Lipowsky, to be published.

[24] Merkel R., Sackmann E. and Evans E., *J. Phys. France* **50** (1989) 1535.

[25] The permeability coefficient of lipid bilayer membranes is known to be of the order of $P = 10^{-5}$ m/s [34]. Converting the hydrostatic pressures to the concentration difference of a solute with the same osmotic pressure, we obtain a net flux of solvent through the membrane $\mathrm{d}Q/\mathrm{d}t = P\Delta p/RT \approx 10^{-14}$ kg /m^{2}s. This is equivalent to a relative velocity of membrane and solvent of 10^{-17} m/s which is totally negligible in comparison with typical membrane velocities of the order $\gamma h \approx 10^{-7}$ m/s. (A similar argument can be found in Youhei F., *Physica A* **203** (1994) 214) If transient pores are created dynamically by shear forces, one has to replace equation (10) by two seperate force balances for the membrane and the solvent at l_0. In the simplest approximation, this gives rise to a q-independent term in γ_s. Only for much higher permeabilities than measured statically one expects measurable effects.

[26] This definition of q_1^f differs from the one given previously in reference [21] by a factor $\kappa/\tilde{\kappa}$ for the sake of better consistency with the respective definition for the case of a bound bilayer.

[27] With $q_2 \simeq 10^9$ m^{-1}, this crossover is of the order of the thickness of the bilayer, where the continuum description may break down.

[28] Pfeiffer W., König S., Legrand J., Bayerl T., Richter D. and Sackmann E., *Europhys. Lett.* **23** (1993) 457.

[29] Israelachvili J., Intermolecular and Surface Forces, 2nd Ed. (Academic Press, London, 1991).

[30] Evans E. and Needham D., *J. Phys. Chem.* **91** (1987) 4219.

[31] Char B.W., Geddes K.O., Gonnet G.H., Leong B.L., Monagan M.B., Watt S.M., Maple V Reference Manual (Springer, Berlin, 1991).

[32] Mutz M. and Helfrich W., *J. Phys. France* **51** (1990) 991.

[33] The unbinding of stacks of membranes has recently been discussed by Netz R.R. and Lipowsky R., *Phys. Rev. Lett.* **71** (1993) 3596;
and by Lipowsky R., *J. Phys.: Cond. Matter*, in press.

[34] Sackmann E., Biophysics, W. Hoppe, W. Lohmann, H. Markl and H. Ziegler Eds. (Springer, Berlin, 1983) pp. 425-457.